# Design and Research of a Novel Multi-Energy Flexible Switching Energy Router

Xu Zai-De, Liu Yang and Zhou Xuguang



October 21, 2019

# Design and Research of a Novel Multi-Energy Flexible Switching Energy Router

XU Zai-de
The Electric Power Research Institute of State Grid Jiangxi Electric Power Ltd
Nanchang，Jiangxi

LIU Yang
The Electric Power Research Institute of State Grid Jiangxi Electric Power Ltd
Nanchang，Jiangxi
Ly_ihuge@163.com

Zhou Xuguang
The Electric Power Research Institute of State Grid Jiangxi Electric Power Ltd
Nanchang，Jiangxi

***Abstract* —On the basis of the flexible access of micro-distributed power supply and hierarchical control of power electronics, design schemes for distributed power supply of energy router and AC/DC load access are proposed. Based on the overall regulation strategy of energy integration, the overall control structure of the energy router is given. Besides, load switching, steady state and switching processes between grid-connected and off-grid are simulated in the Matlab/Simulink environment. The simulation vindicates the feasibility of the control method for each port and the overall control method, which can help satisfy the users’ specific requirements for power quality and can therefore meet the demand.**

***Keywords—energy router, distributed power supply, overall regulation, simulation***

## I. INTRODUCTION

In recent years, power generation devices with distributed renewable energy have been connected into the power grid in quantity, but these new energy power generation methods are often geographically dispersed, intermittent, random and uncontrollable. Additionally, for reducing grid pressure and increasing renewable energy utilization, a large number of energy storage devices are added to the grid to provide buffers for fluctuating energy flows.

In order to accurately quantify the energy from a fixed point and timing, each terminal and node of the power grid need to achieve active scheduling management of energy. Traditional power systems and power equipment often passively adjust power balance, and much difficulties still exist in active control and distribution of power flow. To adapt the complexity and diversity requirements of power grid control in the future, some scholars have proposed to use micro-grid and intelligent community as autonomous units to form the interconnection of energy units from the bottom up.

The research team at North Carolina State University has established a research center for future renewable energy transmission and management systems, aiming to build an efficient distribution network based on renewable energy access and distributed energy storage. Similar to the information router in the computer network, the energy routing device uses the power electronic conversion circuit to control the transformer, and uses the information communication technology to realize the equivalent energy interaction, scheduling, monitoring and distributing the energy flow to ensure the proper access and economical use of the distributed energy.

State Grid Science and Technology Projec(20192BBE50016)

## II. FRAMEWORK DESIGN OF MODULAR ENERGY ROUTER OF DC BUS

The energy router provides access ports for different forms of electrical energy, including input AC ports, output AC ports, and DC ports. Among them, the DC port can be connected to DC devices such as large-capacity energy storage device, distributed power source, and electric vehicle charging device. A total of three DC external ports are provided in the framework, and a dedicated interface for distributed power supply, a dedicated interface for energy storage devices, and a backup interface are provided, as shown in Figure 1.

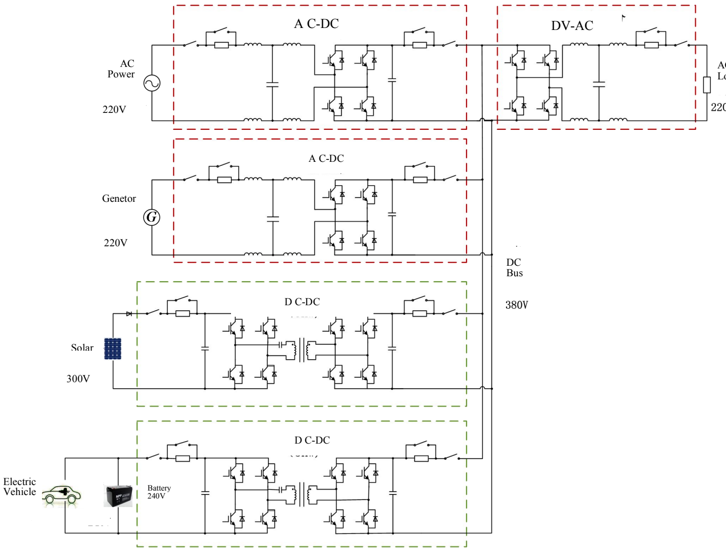


Figure 1. Modular Energy Routing Based on DC Bus

## III. DESIGN OF CORE CONTROLLER

The core control module of the embedded power router mainly includes the main controller STM32F417ZGT, power module, start/reset, 25MHz external crystal oscillator, RS-485 communication interface, human-machine interface, and Ethernet communication interface.

### *A. Controller STM32F417ZGT*

The Cortex-M3 processor adopts Harvard architecture, and the data lines are separated from the address lines to execute instructions while data is being loaded and stored. The STM32F417ZGT features low gate counts, short interrupt latency, and low debug cost. It is designed for deep embedded applications with fast interrupt response requirements. The physical picture of the main control chip is shown in Figure 2:

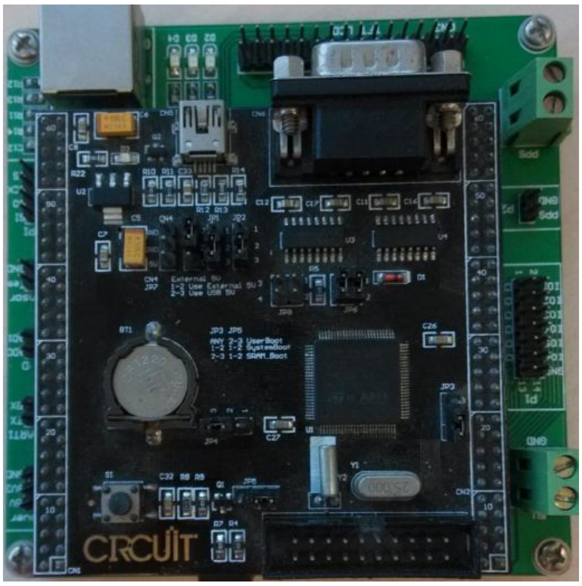

Figure 2: Physical Picture of the Main Control Chip

## B. Power Module

To provide stable power to the main control chip, the power module uses the power supply dedicated chip LM1117 to convert the external 5V power input from the power adapter into the operating voltage of 3.3V required by the STM32F417ZGT. The planar design of the power module is shown in Figure 3.

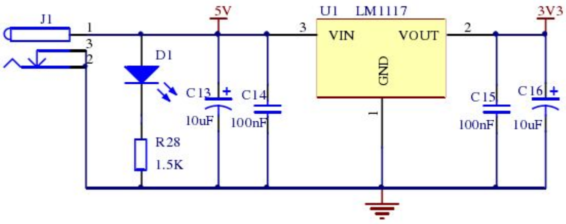


Figure 3. The Planar Design of the Power Module

## C. Choice of Communication Mode between Converters

The function of the energy router's control system is complex, consisting of subsystem units of each stage of the converter. The communication between the units is completed by the CAN bus, and the CAN bus is distributed in the vicinity of the main control unit.

The communication content in the CAN network can be divided into two categories: "main control unit reception" and "main control unit transmission" according to the communication direction. 1) Information received by the main control unit such as bus voltage sample value, output current sample value, peripheral circuit status, peripheral auxiliary device status, and DCS control signal. 2) Information transmitted by the main control unit such as peripheral circuit control signals, auxiliary device control signals, and converter operation data.

## D. Choice of Communication Mode with the Acquisition Module

STM32F417ZGT provides users with various communication interfaces such as I2C interface, USART interface, SPI port and CAN2.0B interface. The RS-485 communication protocol usually uses two transmission lines to support point to multi-point communication. It is half-duplex communication mode containing a single master and multi-slavers, and the maximum rate of data transmission is 10 Mbps.

The connection of bus-type topology of the RS-485 is shown in Figure 4:

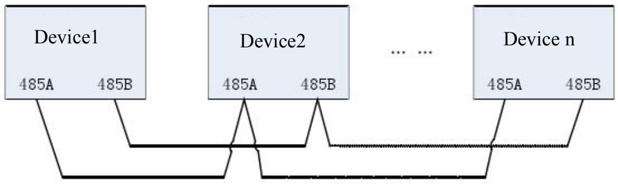


Figure 4: The Connection of Bus-type Topology of the RS-485

## E. Choice of Communication Modes with Other Routers

Communication with other routers adopts the Ethernet communication mode, using the Ethernet dedicated communication chip ENC28J60. The ENC28J60 is an independent Ethernet controller with an industry-standard Serial Peripheral Interface (SPI) that can be used as an Ethernet interface with any controller with SPI. The transmission rate is 10Mb/s. The application circuit of ENC28J60 is shown in Figure 5 below:

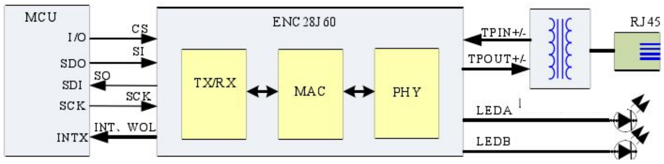


Figure 5. The application circuit of ENC28J60

# IV. .Design and Simulation of Energy Router

## A. Hardware Design of Energy Router

Figure 6 shows the schematic of a power converter used in a 5000W energy router. The power converter shown in the figure can be used as synchronous rectification Buck converter, non-synchronous rectification Buck converter, synchronous rectification Boost converter, non-synchronous rectification Boost converter and Buck-Boost bidirectional converter according to the selection of the input and output ports and the main switching tube.

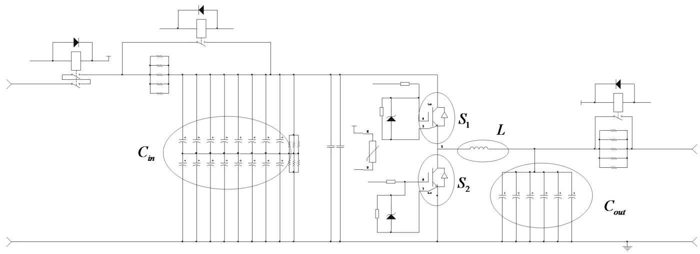


Fig.6 Schematic Diagram of Power Converter of Photovoltaic-Storage Hybrid Power Generation System

## B. System Simulation

In order to verify the effectiveness of the designed energy router, a system simulation model was built in the Matlab/Simulink environment as shown in Figure 7. The main parameters of the energy router simulation model are shown in Table I.

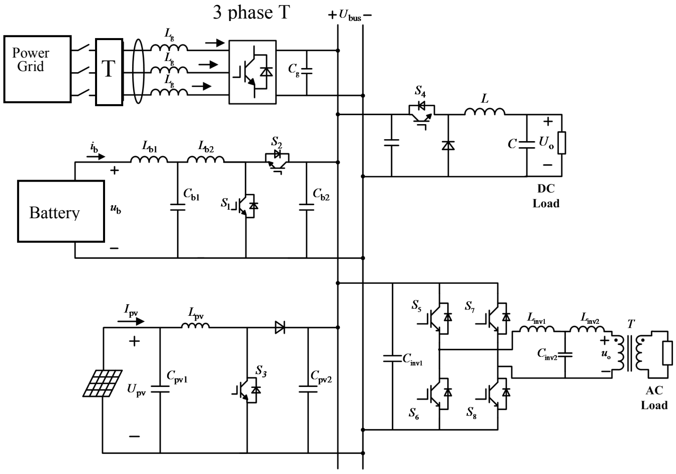


Figure 7 Circuit Structure of the system simulation

TABLE I. THE MAIN PARAMETERS OF THE ENERGY ROUTER SIMULATION MODEL

| Component | Variables and Values |
|---|---|
| Power Grid | phase voltage rms $U = 220\text{V}$, frequency $f$=50Hz , system inductance $L_g = 3\text{mH}$. |
| Photovoltaic | Open circuit voltage and short circuit current are 576V and 15A respectively; The reference temperature is 25℃and the reference light intensity is 1000W/m$^2$; The interface converter is a Boost type circuit structure with a switching frequency of 10kHz, and inductance $L_{\text{inv1}} = 2\text{mH}$. |
| Battery | The interface converter is a bidirectional Buck/Boost circuit structure; In LCL filter link, DC bus side filter inductance $L_{\text{b1}} = 0.5\text{mH}$, filter capacitor $C_{\text{inv}} = 2200\mu\text{F}$, AC output side filter inductance $L_{\text{inv2}} = 2\text{mH}$; Voltage controller proportional coefficient $k_{pu} = 0.01$, integral coefficient $k_{iu} = 1$; current controller proportional coefficient $k_{pi} = 0.1$, integral coefficient $k_{ii} = 0.5$. |
| AC Load | The interface converter is a single-phase inverter full-bridge circuit structure, with 220V rated voltage output; In the LCL filtering link, the DC bus side filter inductance $L_{\text{inv1}} = 0.4\text{mH}$, the filter capacitor $C_{\text{inv}} = 10\mu\text{F}$, and the AC output side filter inductance $L_{\text{inv2}} = 0.2\text{mH}$. |
| DC Load | The interface converter is a Buck type circuit structure, and the output rated voltage is 48V; in the PI voltage controller, the proportional coefficient $k_p = 0.05$ and the integral coefficient $k_i = 10$. |

### C. Working State

#### 1) Steady Operation State

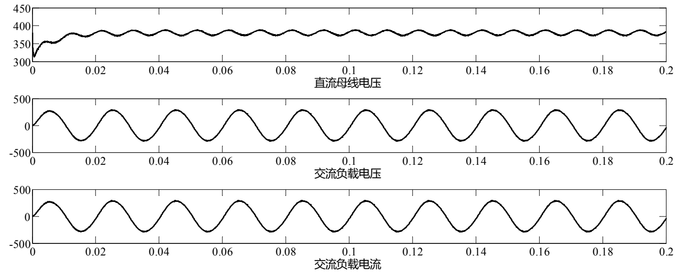


Figure 8. DC Bus Voltage and AC Output Voltage and Current

As shown in Figure 8, the DC bus voltage has a small oscillation around 380V, but after DC-AC conversion, the system can stabilize the AC load.

#### 2) Load Switching Operation Status

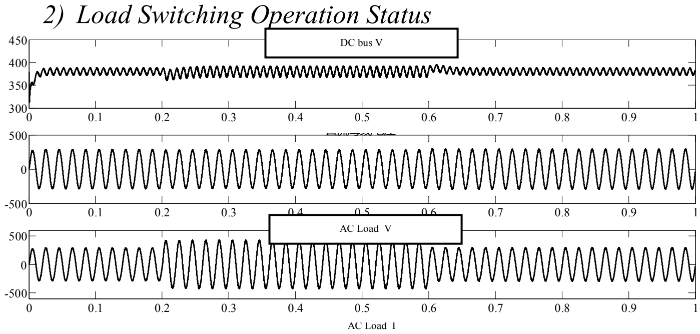


Figure 9 DC Bus Voltage and AC Output Voltage and Current

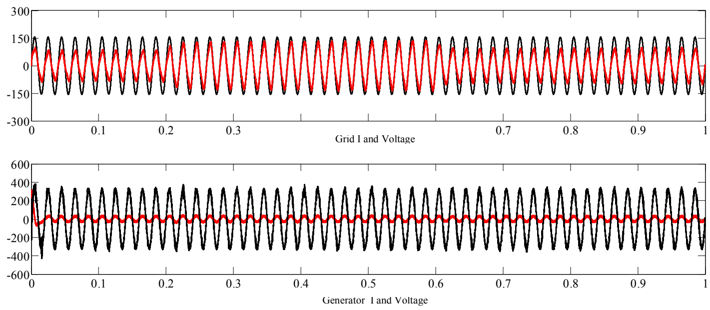


Figure 10: Input Voltage and Current of Large Power Grid and Turbo Generator

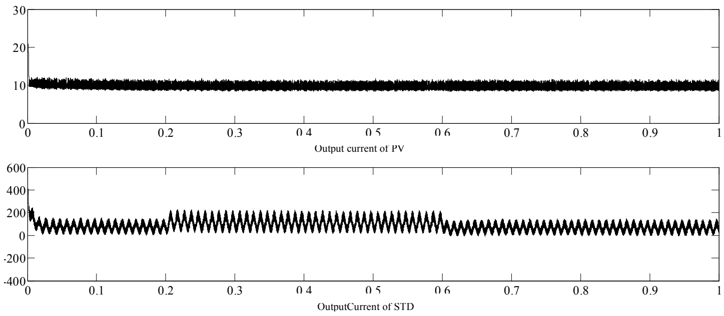


Figure 11 Output Voltage and Current of Photovoltaic Module and Battery Module

It can be seen from Fig. 9 that, when the AC load is input at 0.2s, the DC bus voltage fluctuates slightly, the load voltage is not affected, and the current increases. After the load increases, the input current of the grid side and the battery current increase to energize the load. Photovoltaic and steam turbine generators are not affected, as shown in Figures 10 and 11; after 0.6s, part of the AC load is removed, and the system resumes its initial state and runs stably.

### *3) Grid and Off-Grid Operation Status*

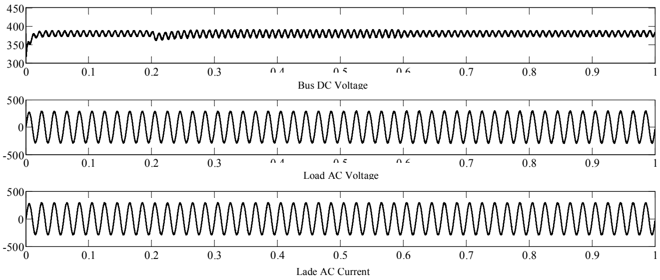


Figure 12 DC Bus Voltage and AC Output Voltage and Current

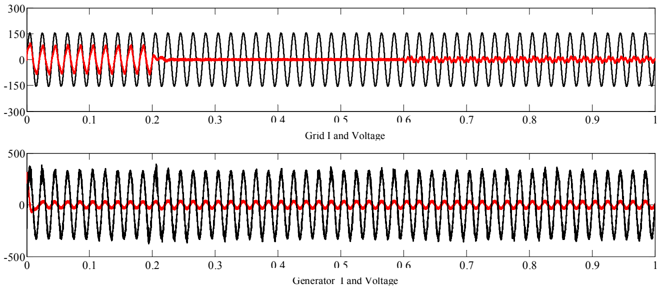


Figure 13: Input Voltage and Current of Large Power Grid and Turbo Generator

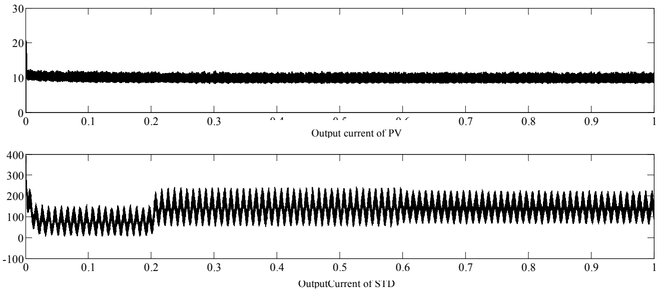


Figure 14. Output Voltage and Current of Photovoltaic Module and Battery Module

At 0.2s, the off-grid operation starts. As can be seen from Figure 12, the DC voltage only slightly fluctuates in the off-network transient state, and the load side voltage and current are not affected. It can be seen from Fig. 13 that, when the AC grid is re-input at 0.6s, with the same load, the energy obtained from the grid side is reduced, and more energy is provided by the distributed power source, which is beneficial to grid-connected operation and will not have any impact on the turbo generator. After shifting into the large grid, the output current of the battery increases, and after the grid is connected again, the current is higher than that before off-grid. As it can be seen from Figure 14, after grid connection, the current of the AC grid side module is reduced, which is beneficial to grid connection. In the process of grid connection and off-grid, the whole system can run stably.

In the simulation process, the system model is firstly constructed according to the energy router topology structure. The overall simulation vindicates that the DC bus voltage stabilizes at 380V, but there is a fluctuation within ±10V. In order to verify the effectiveness of each part of the energy router simulation system, the grid side AC/DC module, the turbine generator AC/DC module, the photovoltaic side DC/DC module and the battery DC/DC module are respectively connected to the AC load through the DC/AC inverter. By analyzing the simulated wave-forms, the constructed energy router can not only maintain a stable load state when all modules are put into operation, but also maintain stability during the switching process of each module, stabilize the DC bus voltage and ensure that the AC load output voltage and current are not affected, and can also run stably during the rise and reduction of the load.

## V. SUMMARY

The energy router is an open energy carrier, which is required to meet the following demands. First, it can not only realize the transformer function, but also provide standardized interfaces for various electric energy forms so that various AC/DC power devices including distributed power generation devices can be connected with the energy router. Additionally, it can control the voltage and current of each port in real time to realize the grid requirements such as energy management and power flow scheduling. It also has satisfactory dynamic characteristics, and is equipped with functions such as dealing with short-circuit faults and completing low-voltage ride through. Furthermore, it can complete the collection of grid data to provide a big data basis for the operation strategy of the energy Internet in a wider range. The energy router proposed in this paper has the function of stabilizing the fluctuation of distributed power output. Through the adjustment function of the system energy control module, the DC bus voltage can be kept basically stable in the off-grid mode and the grid-connected mode. Therefore, the balance between the system power and load-needed power is maintained and power quality meets standard requirements.

## REFERENCES


[1] FAN Ruixiang, DENG Caibo, XU Zaide, et al. A RTDS based APF controller closed-loop simulation method[J]. Automation of Electric Power Systems, 2014, 38(21): 104-107.

[2] XING Shanshan, TIAN Suli, WANG Zhenhua, et al. Optimized design of the voltage controller of PV MPPT system[J]. Power System Protection and Control, 2016, 44(12): 114-118.

[3] ZHOU Jing, BIAN Haifeng, JIA Chen, et al. Real-time reactive power optimization in distribution network with DG based on partitions[J]. Power System Protection and Control, 2015, 43(23): 117-124.

[4] ZHOU Chen, ZHENG Yihui, WANG Xin, et al. Control strategy based on dual-loop controller for split-capacitor- type three-phase four-wire DSTATCOM[J]. Electric Power Automation Equipment, 2014, 34(8): 114-121.

[5] YANG Peihong, LIU Wenying, WEI Yili, et al. Nonlinear excitation control based on adaptive backstepping and variable structure method[J]. Power System Protection and Control, 2012, 40(20): 125-129, 144.

[6] XU Zhengping, LI Jun. Research and implementation of bidirectional full bridge DC-DC converter with high- efficiency control[J]. Power System Protection and Control, 2016, 44(2): 140-146.

[7] WANG He, LI Guoqing. Control strategy of microgrid with different DG types[J]. Electric Power Automation Equipment, 2012, 32(5) : 19-23.

[8] ZHANG Qinjin, LIU Yancheng, WANG Chuan, et al. Study of leakage current suppression method based on NPC photovoltaic grid-connected inverter ［J］ . Electric Machines and Control, 2013, ( 8) : 15-21.

[9] ZHU Fenxin， CHENG Shan， TAN Chao. ZVS isolated high step-up DC／DC converter[J]. Electric Power Aut omation Equipment , 2015， 35(5) : 70-76.

[10] CHENG Chong， ZENG Zheng， TANG Shengqing， etal. Linear optimal control of multi-functional grid-connected inverter[J].Electric Power Automation Equipment， 2016， 36(1) : 135-142.

[11] HOU Nie， SONG Wensheng， WANG Shunliang. Normalization of phase shift control and minimum reflux power control of full-bridge isolated DC/DC converters[J]. Proceedings of the CSEE， 2016， 36（2） : 499-506..